# FAN-BEAM OBSERVATIONS OF RADIO SOURCES AT 21 CM WAVELENGTH

By N. R. Labrum,* T. Krishnan,*† W. J. Payten,* and E. Harting*‡

[*Manuscript received April* 9, 1964]

*Summary*

The compound interferometer at Fleurs, N.S.W., has been used in observations of eight of the strongest radio sources, with a fan beam $1'\cdot53$ wide at a wavelength of $21\cdot1$ cm. Each of the sources was scanned from west to east; the brightness distributions in this direction have been observed, and the positions of the sources in right ascension have been determined with high absolute accuracy (probable error less than 1 s of time).

The results confirm that Centaurus-A, Cygnus-A, and the Omega nebula are all closely-spaced double sources. Sagittarius-A, Taurus-A, Hydra-A, the Orion nebula, and Virgo-A have no fine structure detectable with this angular resolution.

Sagittarius-A is found to be some $8^s$ away from the position given by earlier low resolution observations. In the case of Virgo-A, there is some indication that the radio source is centred in the "jet" rather than in the galaxy. For the other sources, previous identifications are confirmed; the measured right ascensions coincide with the optical objects within the probable-error limits.

## I. Introduction

In a previous paper (Labrum *et al.* 1963—paper A) we described a "compound interferometer" for the observation of galactic and extragalactic radio sources at a wavelength of $21\cdot1$ cm. The aerial system consisted of a long grating array, used as an interferometer in conjunction with a single large aerial (Fig. 1). In the east-west plane, the half-power beamwidth was only $1'\cdot53$; the absolute pointing accuracy

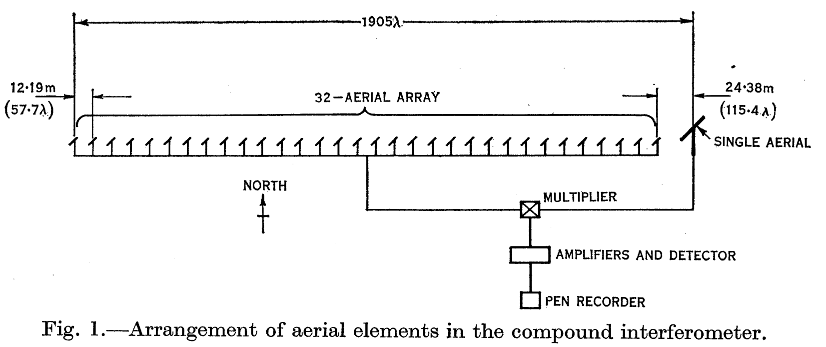


Fig. 1.—Arrangement of aerial elements in the compound interferometer.

was very high (probable error generally less than 1 s of time in right ascension). This is the highest angular resolution yet attained at this wavelength by a direct fan-beam method. The only other fan-beam aerials of comparable beamwidth which have been

* Division of Radiophysics, CSIRO, University Grounds, Chippendale, N.S.W.

† Present address: Stanford Radio Astronomy Institute, Stanford, California, U.S.A.

‡ Present address: Department of Physics, University of New South Wales, Kensington, N.S.W.

used for similar observations are the Pulkovo reflector (beamwidth 2′ at $\lambda = 3\cdot 2$ cm, Khaikin *et al.* 1960) and the Stanford University grating interferometer (2′·3 at 9·2 cm, Little 1963; this instrument has recently been converted to work as a compound interferometer with beamwidth 0′·9, Swarup, Thompson, and Bracewell 1963). The compound interferometer was used to study in detail the brightness distributions of a number of the strongest radio sources, and to determine their positions. The results of these observations are presented and discussed in this paper. We have also included here more detailed discussions of experimental errors, and of the method of data reduction, than were given in paper A.

## II. The Compound Interferometer

### (*a*) *Equipment*

A detailed technical description of the interferometer has already been published (paper A); here a brief specification will suffice. The grating array consisted of 32 equatorially mounted steerable paraboloids, 5·8 m in diameter, spaced at intervals of 12·19 m along an east-west base line (see Fig. 1). The other element of the phase-switched interferometer was a single 18·2 m steerable paraboloid, on an altitude-azimuth mounting. This aerial was sited so that, for transit observations, its electrical centre was 24·38 m (i.e. exactly twice the unit spacing in the array) to the east of that of the easternmost array element.

The receiver had a bandwidth of 7 Mc/s, centred at 1420 Mc/s. The output time-constant was 1 s. In order to avoid the effects of attenuation in the long aerial feeders, a mixer-preamplifier unit was installed at each of the 33 aerials.

### (*b*) *Polar Diagram*

In the north-south plane, the directivity of the instrument was determined by the primary radiation patterns of the aerial elements; the half-power beamwidth in this direction was 53′. The primary directivity of the aerials was sufficient to ensure adequate suppression of all but one at a time of the multiple fan-beam responses (1° apart) of the grating array. Consequently, the east-west polar diagram of the interferometer consisted of a single fan beam; this could be moved in 1° steps by steering the aerials to select successive grating responses. The array aerial feeder-lengths were all accurately equal, so that the zero-order fan beam coincided with the meridian of the station.

The east-west polar diagram (Fig. 2(*a*)) is given by the function $R_{\mathrm{A}}$,

$$R_{\mathrm{A}} \propto \frac{\sin 67x}{\sin x} + C(\theta), \tag{1}$$

where

$$x = \frac{\pi d \sin \theta}{\lambda},$$

$\theta$ = azimuth angle ($\sin \theta \ll 1$), $d$ = unit spacing in array, $\lambda$ = wavelength. $C(\theta)$ is a slowly-varying function of $\theta$; this term is present because of the gap between the large aerial and the end of the array. Over the small angular extent of any of the sources which were studied, $C(\theta)$ is practically constant and merely represents a downward shift in the base line of the record.

$R_A$ exhibits large side lobes, and for a clear presentation of the data it is necessary to smooth the source profiles so that they correspond to a more suitable aerial diagram. It will be shown in the Appendix that this can be done, subject to certain restrictions, by convolving the observed response with a correcting function. The corrected profiles which are presented in this paper correspond to the polar diagram $R_s$ (Fig. 2(b)); this has side lobes less than 4% of the main response, and a half-power width of $1' \cdot 53$.

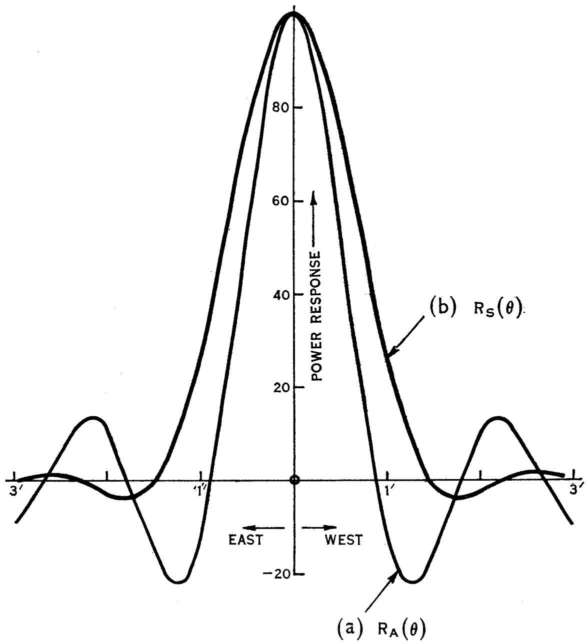


Fig. 2.—East-west directional diagrams for the compound interferometer, showing the received power versus the angular distance of the source from the centre of the fan beam. (*a*) Uncorrected, (*b*) corrected.

## III. Reduction of Data

The deflections on the fan-beam records were read at intervals of time corresponding to changes of 27″ of arc (the "peculiar interval" of the aerial—see Bracewell and Roberts 1954) in the angular position of the source. Corresponding values for from 10 to 16 scans were superimposed for each source, in order to improve the signal-to-noise ratio. A correction was made for the distortion due to the slow response (1 s time-constant) of the recording system. The smoothing process (see Appendix) was then applied to each profile. The smoothed values were plotted as a graph; this gave the convolution of the source brightness distribution with the aerial response $R_s$. The base-line shift due to the gap at the end of the array still remained; the true base line, however, was easily found by inspection.

## IV. Errors

### (a) Position

The factors limiting the accuracy with which the right ascension of a source was determined are as follows:

(i) *Timing Error.*—The combined probable error in setting the sidereal clock (which was checked against WWV time signals before each observation), and in reading the time scale on the record, is estimated to have been $\pm 0^{s}\cdot 2$.

(ii) *Orientation.*—The interferometer base line had been carefully surveyed, and its probable error (deviation from true east-west) was $\pm 4''$.

(iii) *Phasing Errors between Array Elements.*—The relative phases of the signals from the aerials of the grating array had r.m.s. errors (in relation to their mean value) of about 5°. The corresponding probable collimation error was calculated by the procedure used by Mills *et al.* (1958); it was found to be $\pm 7''$.

Table 1

POSITIONS AND SIZES OF SOURCES

| Source | Aerial Declination | Position | | | | Size | |
|---|---|---|---|---|---|---|---|
| | | Epoch of Observation | Observed R.A. h m s | R.A. (epoch 1950·0) h m s | Probable Error (s) | Corrected E-W Half-intensity width (min of arc) | P.E. (min of arc) |
| Sagittarius-A | −28°·9 | 28.viii.62 | 17 43 16·6 | 17 42 28·8 | ±0·8 | 4·1 | ±0·05 |
| Taurus-A | +22°·0 | 28. vi.62 | 05 32 10·0 | 05 31 27·3 | ±0·7 | 3·6 | ±0·05 |
| Centaurus-A* | −42°·8 | 4. vii.62 | 13 23 00·1 | 13 22 16·4 | ±0·9 | 2·1 | ±0·1 |
| | | | 13 23 27·9 | 13 22 44·2 | ±0·9 | 2·7 | ±0·1 |
| Omega nebula | −16°·3 | 19.viii.62 | 18 18 15·6 | 18 17 32·9 | ±0·7 | 4·1 | ±0·05 |
| | | | 18 18 34·0 | 18 17 51·3 | ±1·5 | 2·5 | ±0·15 |
| Orion nebula | −05°·4 | 31.viii.62 | 05 32 25·0 | 05 32 48·9 | ±0·7 | 3·4 | ±0·1 |
| Hydra-A | −11°·9 | 8. ix.62 | 09 16 16·2 | 09 15 41·5 | ±0·7 | 0·5 | ±0·2 |
| Virgo-A | +12°·6 | 5. ix.62 | 12 28 53·4 | 12 28 17·0 | ±0·7 | 1·25 | ±0·15 |
| Cygnus-A† | +40°·6 | 2. ix.62 | 19 58 11·6 | 19 57 44·4 | ±1·0 | — | — |

* Separation in R.A. of the two components = 27·8±0·5 s.

† Position given is for the centre of brightness of the double source.

(iv) *Phasing Error between Array and Large Aerial.*—Because of the geometry of the system, it was necessary to set this phase to correspond to the source declination (see paper A, Section V). In most cases, the probable error in the adjustment is thought to have been about ±10°; this figure corresponds to a collimation error of $\pm 3''$. This phase error is likely to have been somewhat larger for sources observed at very low angles of elevation (see Section V(*h*)).

The summation of these components gives an overall probable error in right ascension of $10''$, or 0·7 s of time, for a source at the celestial equator. The estimated probable error for each source is listed in Table 1.

### (b) *Source Size*

Since all the sources observed had angular widths of the same order as the aerial beamwidth, the observed profile was in every case appreciably broader than the true brightness distribution of the source. In estimating source sizes, an approximate correction for aerial smoothing was applied by using the relation

$$r^2 = a^2+s^2, \tag{2}$$

where $r$, $a$, and $s$ are, respectively, the half-intensity widths of the profile derived from the records; of the polar diagram $R_s$; and of the source brightness distribution. In using this method of correction it was implicitly assumed that both the source brightness and the aerial function $R_s$ could be approximated by one-dimensional Gaussian distributions.

Two other factors made small contributions to the blurring of the profiles. Firstly, errors may have occurred in superposition of successive records, due to timing errors with a probable value of $\pm 0^s \cdot 2$. Secondly, because the receiver had a finite bandwidth, the aerial pattern itself was slightly broadened, except in the zero-order fan beam. As a rule, observations were for this reason restricted to the zero and first-order responses; it is estimated that the broadening of the "average" aerial beam amounted to about 3″. To allow for these effects, a value of $1' \cdot 58$ was adopted for the aerial beamwidth $a$ in equation (2). As has already been mentioned, for a single scan with the zero-order response, $a = 1' \cdot 53$.

## V. Results

The positions and angular sizes of the eight sources which were observed are listed in Table 1, together with the estimated probable errors of the measurements. The observations in each case were spread over about a week; this space of time is not long enough for appreciable precession in right ascension, and the mean epoch is tabulated. The east-west profiles of the sources are shown in Figures 3–10. Our results and conclusions for the individual sources are discussed below. In what follows, all positions quoted are in right ascension for the epoch 1950·0; source widths are corrected for aerial smoothing. On each of the profiles, the r.m.s. level of fluctuations due to receiver noise is indicated by a short vertical line.

### (a) *Sagittarius-A*

The determination of the exact position of this source, which is generally identified with the nucleus of our Galaxy, is a matter of considerable interest, since it has been used to fix the zero of longitude in the new galactic coordinates. In defining this coordinate system, Gum and Pawsey (1960) took the right ascension of Sagittarius-A as $17^h\,42^m\,37^s$. This was based on the mean of several determinations, all of which had been made with comparatively wide-beam aerials (of the order of $0° \cdot 5$). More recent observations with higher angular resolution, however, suggest that this position is several seconds too far to the east (Drake 1959; Little 1963). (On the other hand, Pariiskii (1960) using very narrow fan beams at wavelengths of 3·2 cm and 9·2 cm found a position within $1^s$ of that adopted by Gum and Pawsey.) Drake, who used a 6′ pencil beam at $\lambda = 3 \cdot 75$ cm, was able to show that the intense main source is associated with a complex of weaker but more extended components; thus the low resolution observations would tend to give a false position corresponding to the "centre of gravity" of the whole bright region.

The centre of the main source is found from the present observations to be $8^s$ to the west of the position adopted by Gum and Pawsey. With the exception of Pariiskii's result, all the other narrow-beam measurements agree with our own within the limits of probable error. The strong main source is noticeably asymmetrical, the intensity falling off more rapidly to the east than to the west (Fig. 3). The half-intensity width is $4'\cdot1$.

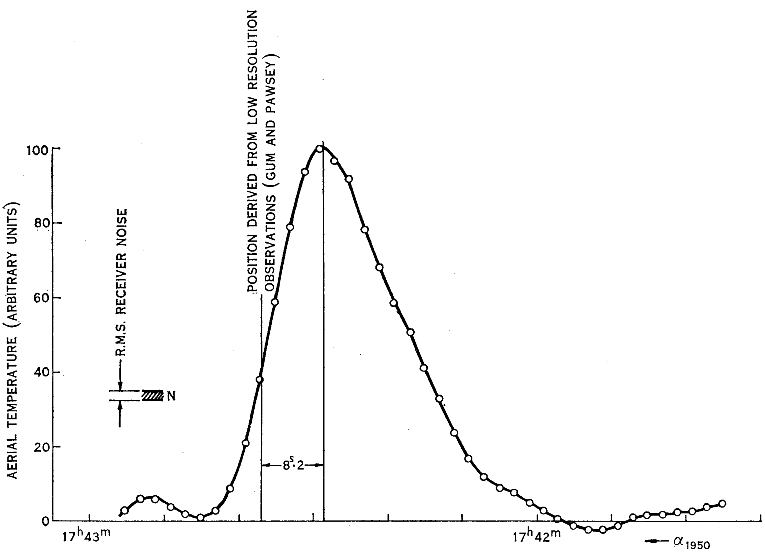


Fig. 3.—Sagittarius-A. In Figures 3–10, the r.m.s. noise level is indicated by the width of the strip marked N.

### (*b*) *Taurus-A* (*Crab Nebula*)

This source (Fig. 4) has a smooth east-west brightness profile, with a width to half-intensity of $3'\cdot6$. This figure agrees closely with an earlier two-aerial interferometer measurement by Twiss, Carter, and Little (1960) at the same wavelength.

The centre of the radio source is about $50''$ to the west of the centre of the optical nebula. A similar displacement is shown by the results of Little (1963) and Pariiskii (1960). The latter points out that the radio centre appears to be in the region of a remarkable variable structure observed by Baade (reported by Oort and Walraven 1956) near the western boundary of the Crab nebula.

### (*c*) *Centaurus-A*

It is well known that this source consists of two large emitting regions, extending over several degrees in declination, with a bright central core (Hindman and Wade 1959). Several high resolution studies have shown that the core is itself a double source (Maltby 1961; Little 1963). Observations with the compound interferometer confirm this result, and provide some further information on the structure of the central part of Centaurus-A.

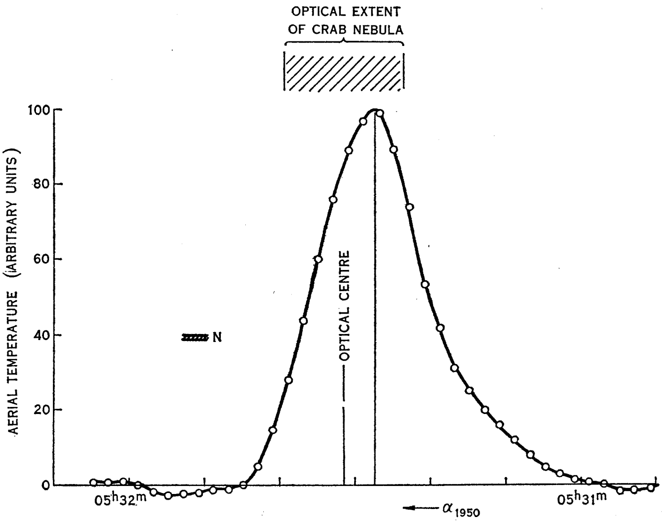


Fig. 4.—Taurus-A.

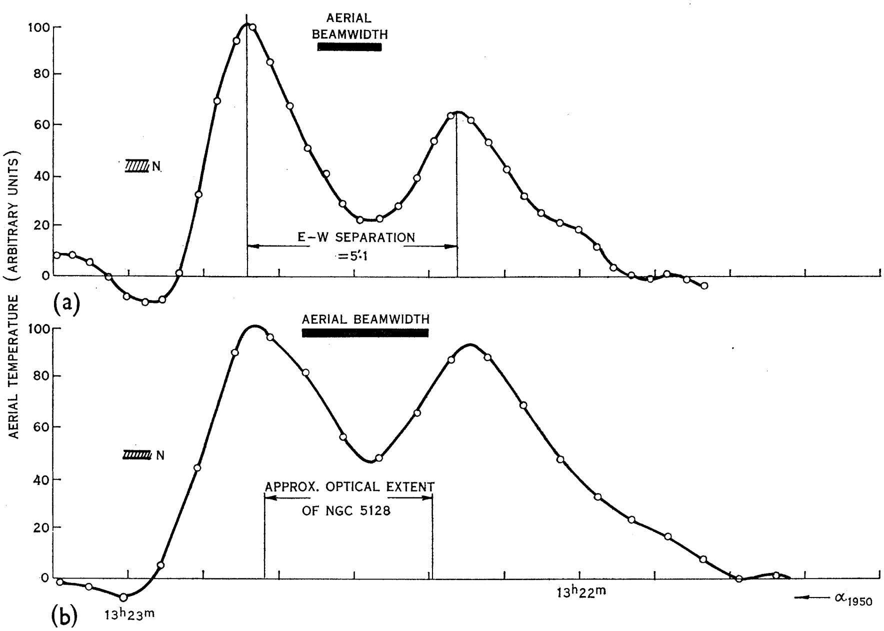


Fig. 5.—Centaurus-A. (*a*) Beamwidth $= 1'\cdot 58$, (*b*) beamwidth $= 3'\cdot 1$.

The profile obtained with the $1'\cdot 58$ fan beam is shown in Figure 5(*a*). The eastern and western sources have widths of $2'\cdot 7$ and $2'\cdot 1$ respectively, whilst their centres are $5'\cdot 1$ apart in the east-west plane.

The components have nearly equal flux densities; this is shown more clearly by Figure 5(*b*), which was obtained by scanning the source with a $3'\cdot1$ fan beam (by using only the eastern half of the array). With this lower resolving power, both components are almost completely unresolved, so that the peak ordinates of the curve are proportional to the flux densities. These ordinates differ in height by less than 10%. The profiles agree closely, in source size, spacing, and relative intensity, with a model which Maltby derived from two-aerial interferometer measurements ($\lambda = 31\cdot3$ cm). At $9\cdot2$ cm wavelength, Little found a somewhat different brightness distribution, with the flux densities of the two components in the ratio of $1\cdot0 : 0\cdot57$, the eastern source being the stronger. The possibility of a real variation with wavelength cannot be excluded; it appears, however, that at least part of the discrepancy is due to the fact that Little estimated that the western source was only $1'\cdot1$ wide. The present observations with the $1'\cdot58$ beamwidth make it clear that, at least at $\lambda = 21\cdot1$ cm, both components have east-west widths between $2'$ and $3'$.

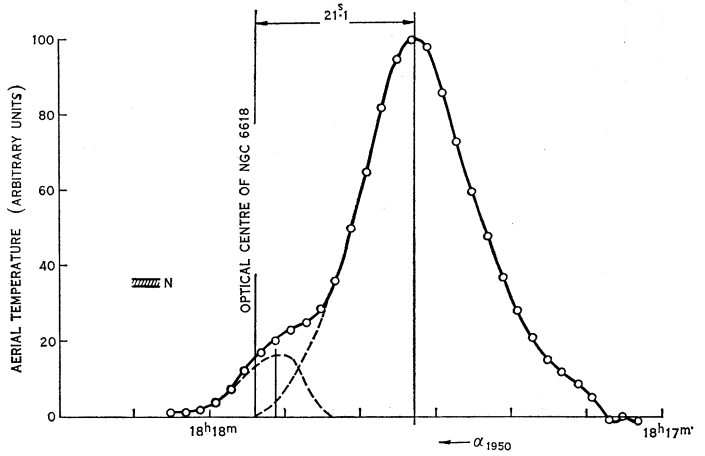


Fig. 6.—Omega nebula. The broken lines show the estimated responses to the two components of the source.

The right ascension of each component is given in Table 1. The two sources are spaced fairly symmetrically east and west of the galaxy NGC 5128 (Fig. 5). Little gives positions which differ from ours by several seconds of time in each case. This disagreement is rather larger than would be expected from the estimated probable errors; the resulting uncertainty, however, is too small to affect the general conclusion as to the relative positions of the optical galaxy and the radio sources.

### (*d*) *The Omega Nebula* (*NGC* 6618)*

The brightness profile obtained for this source is shown in Figure 6. The peak radio intensity is at R.A. $18^{h}\,17^{m}\,32^{s}\cdot9$; this is some $21^{s}$ west of the centre of the optical object (Cederblad 1946), and is, in fact, close to the western boundary of the nebula as shown on photographs.

* A detailed analysis of all the available data on this source will be published in the near future (T. Krishnan, in preparation).

The observations show clearly that the source is complex. There is a conspicuous "bump" on the eastern side of the profile; this can best be interpreted as the effect of a second and much weaker component of the source. The main peak has a half-intensity width of $4' \cdot 1$; if its profile is assumed to follow a smooth curve (broken line in Fig. 6), the smaller component is found to be located about $18^s$ further east, and to be $1' \cdot 6$ wide. The ratio of flux densities is about 10 : 1; the smaller source is located very near the right ascension of the optical centre of the nebula. Little (1963) found evidence at $\lambda = 9 \cdot 2$ cm of a subsidiary source in about the same position as that shown in Figure 6; in this case the ratio of flux densities was $3 \cdot 7$ : 1. Pariiskii (1960) obtained a profile of the Omega nebula at $\lambda = 9 \cdot 4$ cm, which appears to indicate a similar double structure; however, he does not comment on the possible presence of a second component.

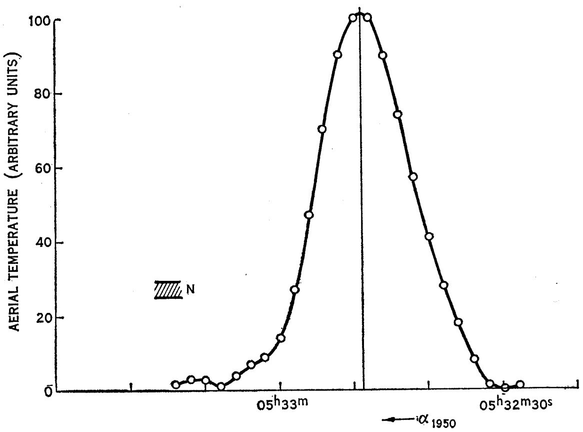


Fig. 7.—Orion nebula.

The second source is no more clearly resolved in our observations than in Little's, in spite of our narrower beamwidth ($1' \cdot 58$ against $2' \cdot 3$). It appears, therefore, that the two sources actually overlap in the east-west plane; it would now be of great interest to examine the Omega nebula with an instrument having high north-south resolution.

## (e) *The Orion Nebula*

Menon (1961), Pariiskii (1961*a*), and Little (1963) have all concluded that the position of this radio source coincides with $\theta^{\mathrm{I}}$ Orionis, the exciting stars of the Orion nebula. The present measurement confirms this identification; the position of peak intensity is within $0^s \cdot 2$ of the mean R.S. of $\theta^{\mathrm{I}}$ Orionis (Strand 1958).

The source was found to have a smooth radio brightness distribution, with a half-intensity width of $3' \cdot 1$ (Fig. 7). It is slightly asymmetrical, extending further to the east than to the west of its peak. These results agree closely with the work of Menon at $\lambda = 3 \cdot 75$ cm; Little at $9 \cdot 2$ cm; and Twiss, Carter, and Little (1960) at $21 \cdot 2$ cm. Pariiskii, however, gives a source width of only $2' \cdot 4$ at $8 \cdot 5$ cm.

*(f) Hydra-A*

This source has been identified with a close double galaxy in cluster A780 (Mills 1960; Roberts, Bolton, and Harris (1960). The present measurements are in good agreement with this identification; the optical galaxy is at R.A. $09^h 15^m 41^s \cdot 2$, which differs from the $21 \cdot 1$ cm radio position (Table 1) by an amount less than the probable error of the latter.

The observed response curve (Fig. 8) has a half-power width of only $1' \cdot 66$. This is so close to the effective aerial beamwidth that the source size cannot be accurately determined. The most probable value for the equivalent width is found to be $0' \cdot 5$.

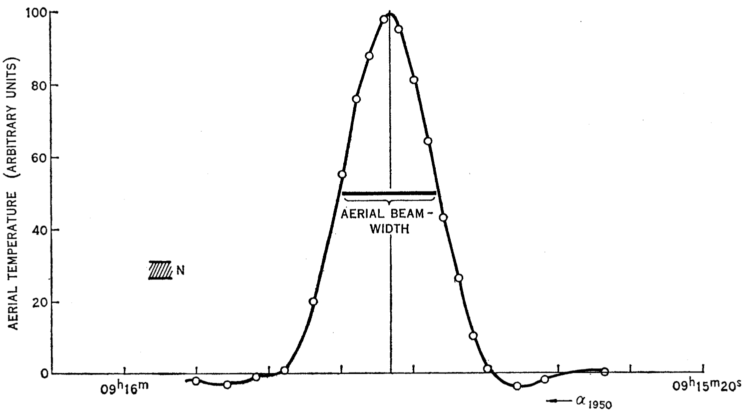


Fig. 8.—Hydra-A.

*(g) Virgo-A*

The observed profile is shown in Figure 9(*a*). After correction for aerial smoothing, the source width to half-intensity was found to be ($1' \cdot 25 \pm 0' \cdot 15$). This result is compatible with the brightness distribution deduced by Lequeux (1962), which consists of two components 23″ wide and 31″ apart in the east-west plane. The angular resolution of the compound interferometer was too low to give an indication of any fine structure within the source.

Shklovskii (1955) suggested that the radio emission from this source originates as synchrotron radiation from the "jet", a structure which extends some 20″ westwards from the optical centre of the galaxy M87. Obviously this hypothesis can be tested by an accurate measurement of the relative positions of the optical and radio sources.

The observations with the compound interferometer placed the centre of the radio source very slightly ($0^s \cdot 65$) west of the centre of the nucleus of M87 (using accurate optical positions listed by Griffin (1963)). This displacement is, however, less than the probable error, and cannot in itself be regarded as significant. Little's measurements agree closely with our own; several other workers have found positions further to the west, i.e. away from the galaxy. These results are shown in Figure 9(*b*). In every case, the probable error is comparable with the observed displacement from the optical centre of the galaxy. However, since all the observations agree qualitatively in giving a westwards displacement, it seems safe to conclude that the radio emission is, in fact, associated with the jet rather than with the nucleus of the galaxy.

### (*h*) *Cygnus-A*

Observations of Cygnus-A were made under unfavourable conditions, owing to its low elevation above the northern horizon ($15\frac{1}{2}°$ at meridian transit). Tropospheric refraction had an appreciable effect upon the apparent declination of the

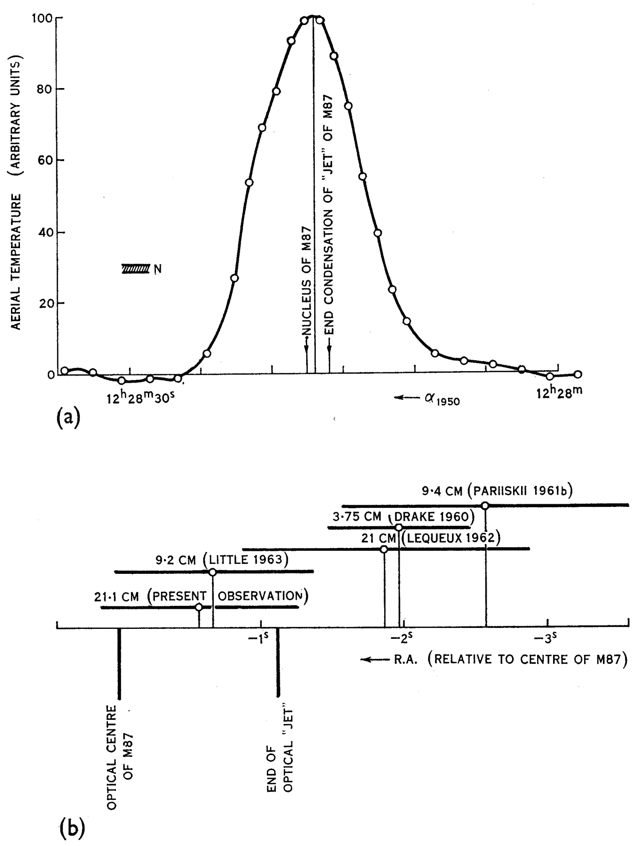


Fig. 9.—Virgo-A. (*a*) East-west profile. (*b*) A comparison of optical and radio measurements of position. The horizontal bars indicate probable-error limits.

source, and so on the relative phases of the signals from the array and from the single-aerial element. It was in fact found that the phase changed slightly from night to night, and that it was necessary on each occasion to estimate the phase error from the appearance of a preliminary scan across the source. An empirical phase correction was then made before the beginning of the main part of the record. Because of this complication the positional accuracy is rather lower than for the other sources; it is also possible that residual phase errors may have caused some slight distortion of the profile.

Many previous observations have shown that this source is double (e.g. Jennison and Latham 1959; Lequeux 1962). Both Lequeux and, more recently, Swarup, Thompson, and Bracewell (1963), have found that the space between the main components of the doublet appears to be bridged by a broader and weaker source. The resolving power of the compound interferometer was not quite sufficient to show these structural details explicitly; an approximate picture of the source has, however, been derived by comparing the observed profile with the calculated responses to various assumed brightness distributions.

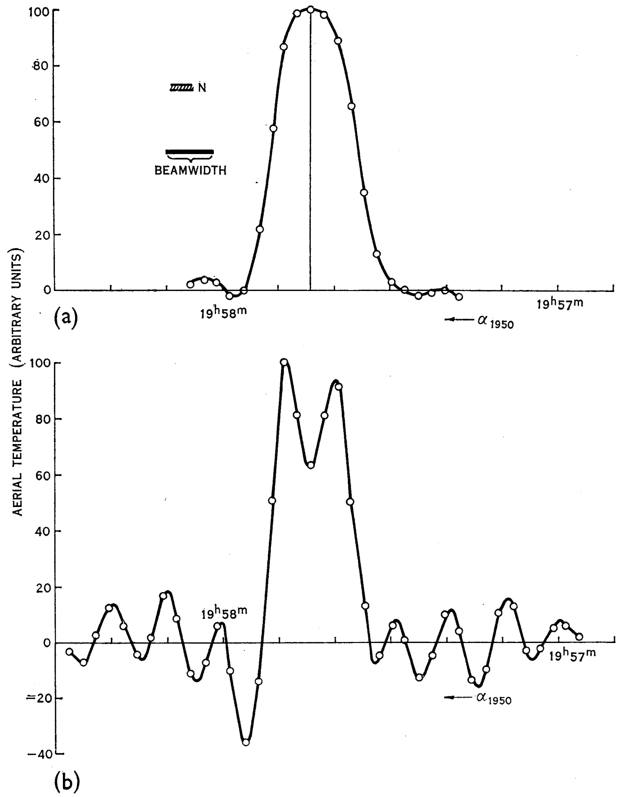


Fig. 10.—Cygnus-A. (*a*) Corrected response, (*b*) uncorrected response.

This comparison could, in principle, be carried out with the smoothed profile (Fig. 10(*a*)). It was, however, somewhat more convenient to convolve the model distributions with the uncorrected polar diagram in Figure 2(*a*), and to compare the results with the corresponding observed profile (Fig. 10(*b*)). The latter is almost symmetrical, and as a further simplification we have considered only symmetrical models. Accordingly, the experimental curve in Figure 11 was obtained by averaging the two halves of Figure 10(*b*). Figure 11 shows the best fit with experiment for two equal point sources; for a uniformly bright strip; and for a distribution consisting of two equal point sources joined by a uniform strip. In the first two cases the fitting was done by adjusting the source width; the composite source was fitted by varying both the overall width and the relative intensities of the components.

It is apparent from the diagram that the uniform-strip model is inadmissible. Both the other distributions, however, can be adjusted to fit the observations (with different values for the source width). We conclude therefore that the source has two main components which are both too narrow in the east-west plane to be resolved by the interferometer; and that the angular resolution is too low to establish whether or not a more extended component is also present.

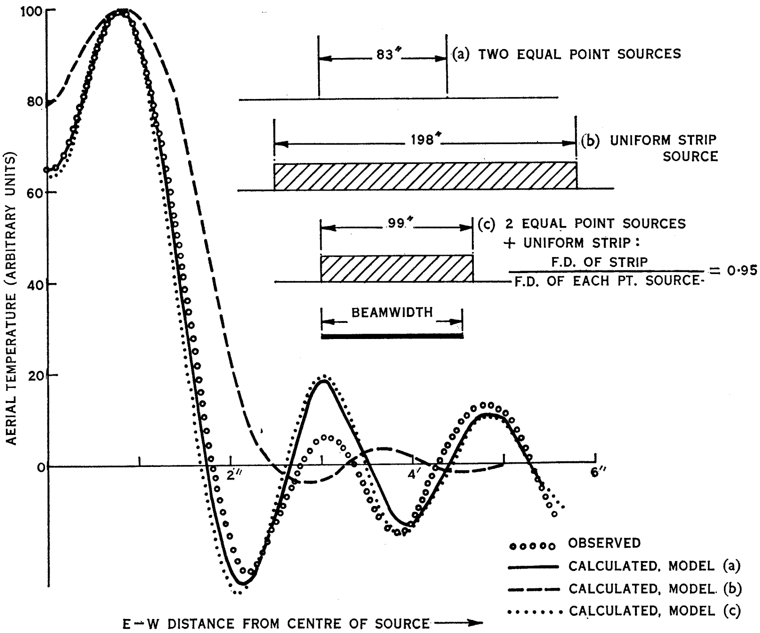


Fig. 11.—Cygnus-A observations compared with three best-fit model responses. The brightness distributions used for the source models are indicated at the right.

In the case where an extended component is included in the model (see Fig. 11) the east-west spacing of the doublet is found to be 99″. This agrees very well with the work of Swarup, who found that all the available evidence can be explained if Cygnus-A consists of a pair of sources 101″ apart joined by a more extended bright region.

Within the probable-error limits, the right ascension of the centre of Cygnus-A coincides with that of the optical object with which the source was identified by Baade and Minkowski (1954). The present measurement thus provides further confirmation of an already well-established identification.

## VI. Acknowledgments

Thanks are due to Messrs. J. Palmer, G. Fairweather, and C. Turrall for their assistance in making the observations; and to Mrs. B. M. Sullivan who carried out most of the work of data reduction.

One of us (T.K.) wishes to thank the Federal Government of Australia for extending its hospitality to him under the Colombo Plan.

We are greatly indebted to Professor W. N. Christiansen and to the late Dr. J. L. Pawsey for their helpful advice at all stages of this work and for their constant interest and encouragement.

## VII. References

Baade, W., and Minkowski, R. (1954).—*Astrophys. J.* **119**: 206.
Bracewell, R. N., and Roberts, J. A. (1954).—*Aust. J. Phys.* **7**: 615.
Cederblad, S. (1946).—*Publ. Lund. Obs.* **119** (2): 120.
Drake, F. D. (1959).—Annual Rep. Nat. Radio Astr. Obs., U.S.A.
Drake, F. D. (1960).—Annual Rep. Nat. Radio Astr. Obs., U.S.A.
Griffin, R. F. (1963).—*Astr. J.* **68**: 421.
Gum, C. S., and Pawsey, J. L. (1960).—*Mon. Not. R. Astr. Soc.* **121**: 150.
Hindman, J. V., and Waade, C. M. (1959).—*Aust. J. Phys.* **12**: 258.
Jennison, R. C., and Latham, V. (1959).—*Mon. Not. R. Astr. Soc.* **119**: 174.
Khaikin, S. E., Khaidanovsy, N. L., Esepkina, N. A., and Shivris, O. N. (1960).—*Izv. G.A.O. Pulkovo* **21** (5): 27.
Labrum, N. R., Harting, E., Krishnan, T., and Payten, W. J. (1963).—*Proc. Inst. Radio Engrs. Aust.* **24**: 148.
Lequeux, J. (1962).—*Ann. Astrophys.* **25**: 221.
Little, A. G. (1963).—*Astrophys. J.* **137**: 164.
Maltby, P. (1961).—*Nature* **191**: 793.
Menon, T. K. (1961).—*Publ. Nat. Radio Astr. Obs.*, U.S.A., Vol. 1, No. 1.
Mills, B. Y. (1960).—*Aust. J. Phys.* **13**: 550.
Mills, B. Y., Little, A. G., Sheridan, K. V., and Slee, O. B. (1958).—*Proc. Inst. Radio Engrs.* 46: 67.
Oort, J. H., and Walraven, T. (1956).—*Bull. Astr. Insts. Neth.* **12**: 285.
Pariiskii, Y. N. (1960).—*Izv. G.A.O. Pulkovo* **21** (5): 45.
Pariiskii, Y. N. (1961a).—*Astr. Zh.* **38**: 798.
Pariiskii, Y. N. (1961b).—*Doklady Akad. Nauk S.S.S.R.* **137**: 49.
Roberts, J. A., Bolton, J. G., and Harris, D. E. (1960).—*Publ. Astr. Soc. Pacif.* **72**: 5.
Shklovskii, I. S. (1955).—*Astr. Zh.* **32**: 215.
Sloanaker, R. M., and Nichols, J. H. (1960).—*Astr. J.* **65**: 109.
Strand, K. A. (1958).—*Astrophys. J.* **128**: 14.
Swarup, G., Thompson, A. R., and Bracewell, R. N. (1963).—*Astrophys. J.* **138**: 305.
Twiss, R. Q., Carter, A. W. L., and Little, A. G. (1960).—*Observatory* **80**: 153.
Wild, J. P. (1960).—*Proc. Roy. Soc.* A **262**: 84.

## Appendix

### *Correction of the Compound Interferometer Polar Diagram*

The polar diagram of the interferometer is given (apart from a displacement of the base-line) by equation (1) (see Section II($b$))

$$R_{\mathrm{A}}(\theta) \propto \frac{\sin \dfrac{67\pi d\theta}{\lambda}}{\sin \dfrac{\pi d\theta}{\lambda}}. \tag{A1}$$

Because this function has large side lobes, patterns recorded directly do not present the source brightness distribution in an easily intelligible form. However, the data can be used to obtain the response corresponding to a more suitable polar diagram.*

Let a source with one-dimensional brightness distribution $S(\theta)$ be scanned by a fan-beam aerial with a response pattern $R(\theta)$. The received signal $P(\theta)$ is given by the convolution

$$P(\theta) = R(\theta) * S(\theta). \tag{A2}$$

From the convolution theorem,

$$\overline{P}(u) = \overline{R}(u).\overline{S}(u), \tag{A3}$$

where $u$, the "spatial frequency", is a coordinate measuring distance along the aperture plane of the aerial; $\overline{P}(u)$ is the Fourier transform of $P(\theta)$, and so on.

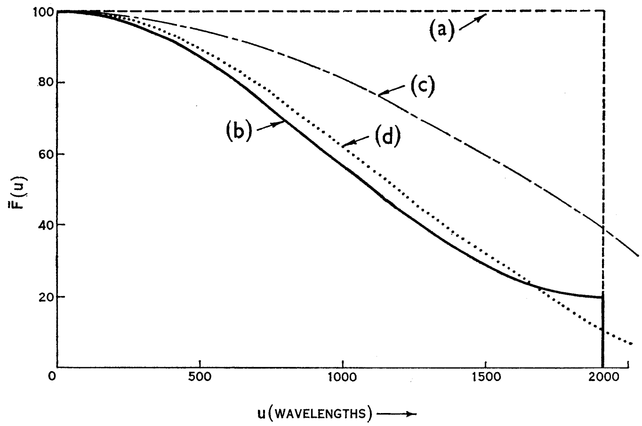


Fig. 12.—Spatial frequency spectra of aerial patterns. (*a*) Uncorrected polar diagram of interferometer; (*b*) a polar diagram which is known to have low sidelobes ($R_1(\theta)$, Fig. 13(*b*)); (*c*) 3-point correcting function; (*d*) 5-point correcting function.

If the same source distribution is scanned by an aerial with polar diagram $R'(\theta)$, the response $P'(\theta)$ is given by

$$P'(\theta) = R'(\theta) * S(\theta), \tag{A4}$$

$$\overline{P}'(u) = \overline{R}'(u).\overline{S}(u), \tag{A5}$$

hence

$$\overline{P}'(u) = \overline{P}(u).\overline{R}'(u)/\overline{R}(u), \tag{A6}$$

and

$$P'(\theta) = P(\theta) * F(\theta), \tag{A7}$$

where

$$\overline{F}(u) = \overline{R}'(u)/\overline{R}(u). \tag{A8}$$

Thus, the correction process consists of convolving the observed source profiles

* This method of polar-diagram correction has been described by Wild (1960), who considered the more general case of a two-dimensional diagram.

with a correcting function $F(\theta)$; the latter is specified in terms of the polar diagrams by equation (A8). This result is valid if the corrected aerial response $R'(\theta)$ contains no spatial frequency components which are missing from the original response $R(\theta)$; i.e. if $\bar{R}'(u)$ is zero at all values of $u$ for which $\bar{R}(u)$ is zero.

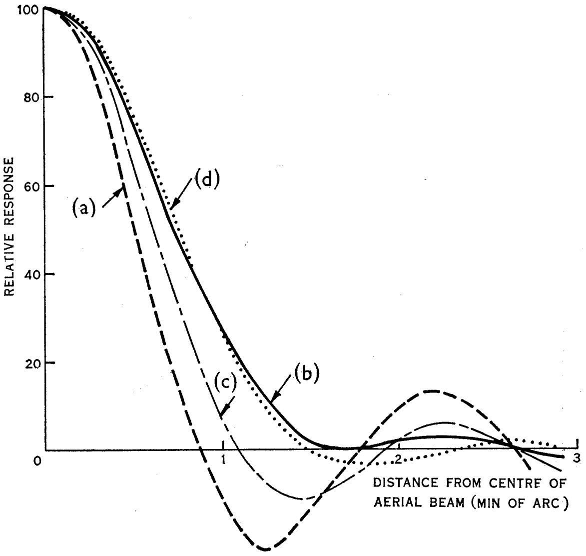


Fig. 13.—Calculated point source responses. ($a$) Compound interferometer without correction; ($b$) the polar diagram $R_1(\theta)$; ($c$) compound interferometer corrected with 3-point function; ($d$) compound interferometer corrected with 5-point function.

In the present case, $R(\theta)$ is the response of the compound interferometer ($R_A(\theta)$ in equation (A1)). The corresponding spatial frequency spectrum $\overline{R_A}(u)$ has constant amplitude up to a cut-off frequency, beyond which it is zero (Fig. 12($a$)).

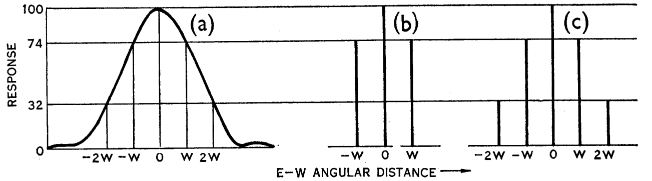


Fig. 14.—Illustration of the method of deriving 3-point ($b$) and 5-point ($c$) correcting functions from the function $R_1(\theta)$ shown at ($a$). $w$ is the peculiar interval for the interferometer.

This simplifies the method of correction, since it follows from equation (A8) that the correcting function $F(\theta)$ is in this case identical with the corrected aerial response $R'(\theta)$. For the latter, the function $R_1(\theta)$ (Fig. 13($b$)) was selected. Its spectrum $\overline{R_1}(u)$ is shown in Figure 12($b$).

All the information can be extracted from the records by sampling the latter at intervals equal to the "peculiar interval" of the aerial (Bracewell and Roberts 1954). It is therefore desirable, for ease of computation, to replace the correcting function $R_1(\theta)$ by a set of values corresponding to discrete points which are also spaced at the peculiar interval.

The suitability of 3-point and 5-point correcting functions (Fig. 14) was first investigated by comparing their Fourier transforms with the spatial frequency spectrum $\overline{R_1}(u)$. As an additional check, the point-source response was computed in each case. The results are summarized in Figures 12 and 13. It is clear that the 5-point and continuous functions give almost identical responses up to the spatial cut-off frequency but that the 3-point convolution leads to a much poorer approximation.

All the observations discussed in this paper have been smoothed by use of the 5-point correcting function. The source profiles, therefore, correspond to the aerial pattern of Figure 13($d$), which is reproduced as $R_s$ in Figure 2($a$).